International Journal of Chemical, Materials and Biomolecular Sciences
ISSN: 2415-6620
Vol:10, No:7, 2016

Influence of Argon Gas Concentration in N_2-Ar Plasma for the Nitridation of Si in Abnormal Glow Discharge

K. Abbas, R. Ahmad, I. A. Khan, S. Saleem, U. Ikhlaq

***Abstract*—**Nitriding of p-type Si samples by pulsed DC glow discharge is carried out for different Ar concentrations (30% to 90%) in nitrogen-argon plasma whereas the other parameters like pressure (2 mbar), treatment time (4 hr) and power (175 W) are kept constant. The phase identification, crystal structure, crystallinity, chemical composition, surface morphology and topography of the nitrided layer are studied using X-ray diffraction (XRD), Fourier transform infra-red spectroscopy (FTIR), optical microscopy (OM), scanning electron microscopy (SEM) and atomic force microscopy (AFM) respectively. The XRD patterns reveal the development of different diffraction planes of Si_3N_4 confirming the formation of polycrystalline layer. FTIR spectrum confirms the formation of bond between Si and N. Results reveal that addition of Ar into N_2 plasma plays an important role to enhance the production of active species which facilitate the nitrogen diffusion.

***Keywords*—**Crystallinity, glow discharge, nitriding, sputtering.

I. Introduction

THE Si_3N_4 thin films show remarkable properties which make them suitable in various applications due to their diverse properties such as high mechanical strength; dielectric constant; excellent chemical stability; good resistance to wear and corrosion; thermal shock and creep. Hence, the Si_3N_4 films are used as passivation layers, alkali–ion diffusion barrier, gate dielectrics, oxidation mask, hard coating materials and in high-temperature applications [1]-[3]. The Si_3N_4 films are synthesized through different routes like direct nitridation of silicon [4], activated reactive evaporation (ARE) [5], chemical vapor deposition (CVD) [6], plasma-enhanced chemical vapor deposition (PECVD) [7], laser-assisted CVD [8], DC reactive magnetron sputtering [3] and plasma focus device [9].

Plasma nitriding has attracted much attention because it is environmentally-friendly technique. A pulsed DC discharge is preferable over conventional DC discharge due to its operation at relatively high peak voltages and currents for the same average power as compared to conventional DC glow discharge which leads to increase the ionization, excitation and sputtering processes [10]. Plasma generated by only N_2 gas is not suitable because its dissociation efficiencies are about 2% which is due to highly stable bonding between N_2 species. One promising way to enhance the dissociation of N_2 in plasma is to introduce the inert gases like Ar, neon and helium [11]. It is well known that addition of Ar in N_2 plasma enhances the electron temperature, electron number density, concentration of active species through Penning excitation and ionization [12], [13]. Moreover, it is noticeable that the addition of Ar in N_2 plasma serves as a catalyst enhancing the concentration of active species of N_2 and increasing the reactivity of silicon with N_2 plasma species to form nitrides [14], [15].

The present work highlights the importance of sputtering gas (Ar) concentrations on the kinetics of layer growth. Structural, morphological and compositional properties of the nitrided layer are examined in terms of their crystal structure, chemical bonding, and surface morphology. The role of sputtering gas on crystallite size and residual stress of silicon nitrided thin films is also investigated.

K. Abbas is PhD scholar at Department of Physics, GC University, Lahore, 54000, Pakistan (corresponding author, phone: 0046764227525; email: Khizra_11@hotmail.com).

R. Ahmad (Chairman of Department of Physics and Director of Centre for Advanced Studies in Physics), S. Saleem (PhD scholar), and U. Ikhlaq (PhD scholar) are with the Department of Physics, GC University, Lahore, 54000, Pakistan.

I. A. Khan (Assistant Professor) is with the Department of Physics, GC University, Faisalabad, 38000, Pakistan.

II. Experimental Setup

In order to study the influence of Ar concentration in N_2-Ar plasma on the nitrided layer properties, the Si samples are nitrided in a stainless steel chamber by using pulsed DC glow discharge technique. Fig. 1 shows the schematic arrangement of pulsed DC glow discharge system. The chamber consists of two movable parallel electrodes having a diameter of 9.5 cm and thickness of 1.9 cm. The upper electrode serves as anode, whereas the lower electrode serves as cathode (sample holder). The chamber is evacuated down to 10^{-2} mbar pressure by using rotary vane pump prior to filling the N_2-Ar gases. The inter-electrode distance (3 cm), pressure (2 mbar) & power (175 W) are kept constant throughout the experiment.

By applying pulsed-DC power to the upper electrode (anode), glow discharge is produced. The pulsed DC power is obtained by using 50 Hz AC power source, step-up transformer and bridge rectifier. The plasma is excited in an abnormal glow regime using various ratios of Ar & N_2.

To control the input current and voltage within the discharge, voltmeter and ammeter are used. There is no need of auxiliary heater as the sample is being heated up by the bombardment of cathodic energetic atoms, molecules, ions and radicals of N_2 which may be controlled by increasing the Ar concentration in N_2-Ar plasma.

Silicon substrates having dimension 1cm × 1cm and thickness 0.3 mm are placed on the cathode (substrate holder)

for 4 hrs processing time using various concentrations of N_2-Ar plasma. The untreated Si and nitrided Si samples are characterized by XRD, FTIR, OM, SEM and AFM in order to investigate the structural, morphological and surface roughness of the silicon nitride layers.

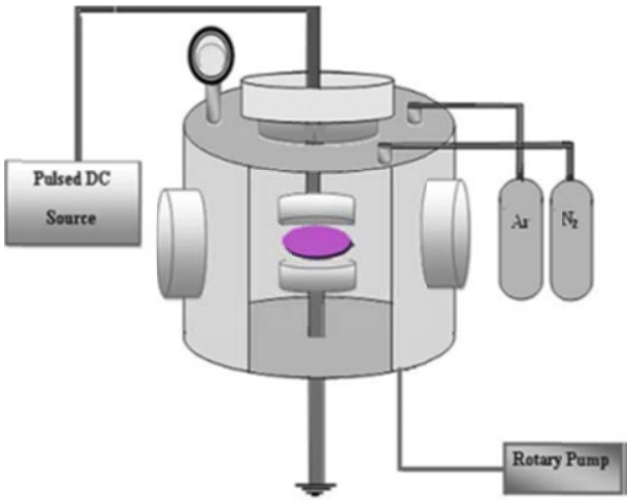

Fig. 1 A schematic diagram of pulsed DC glow discharge system

III. Results and Discussion

A. XRD Analysis

Figs. 2-4 show the XRD patterns of untreated Si and nitrided Si samples for different Ar concentration in N_2-Ar plasma by keeping the other discharge parameters constant. The XRD pattern of untreated Si shows a single intense diffraction peak corresponding to Si (100) orientation as shown in Fig. 2 (a).

Fig. 2 (b) shows the development of two diffraction peaks showing weak intensities related to Si_3N_4 (301) & (204) planes along with a broad diffraction peak of (103) plane. The peak intensity of Si (100) is drastically decreased showing a broad hump, which indicates the amorphization of Si. It is reported that crystallite size is inversely proportional to peak broadening. Thus, the broadened peaks exhibit the formation of nano-crystallites of Si_3N_4 which are due to the bombardment of N active species as well as their infusion in Si lattice.

The peak intensity of Si_3N_4 phase growing along different (301), (204) & (103) orientations increases up to 60% argon, which starts to decrease for 70% to 90% Ar contents. This indicates that Ar contents greater than 60% is not favorable for the growth of Si_3N_4 but re-sputtered the previously deposited nitrided layer. Moreover, lower nitrogen content or higher substrate temperature hinders the nucleation of silicon nitride along other orientations. For 90% argon, no diffraction peak is observed thereby confirming the formation of amorphous film.

It has been reported that electron temperature increases by the addition of argon gas [16], [17]. This may be owing to lower electron collision cross-section of Ar as compared to N_2 that provides adequate time for electrons to be accelerated in the electric field and results in high energy electrons. These energetic electrons may directly ionize and excite nitrogen molecules or bring Ar to its metastable states. As a result, it may collide with nitrogen molecules and ionize and excite them. Hence, Penning excitation and ionization event enhance active species concentration in the discharge. Energetic argon ions cause more sputtering of target material in comparison to nitrogen ions, which increases the discharge current [18], [19].

The argon contents and energies influence the discharge current which is responsible for the growth of nitride layer. The argon gas also contributes in molecular dissociation of nitrogen through electron-molecule impact dissociation, heavy particles-molecules impact and heavy particle-solid surface impact [20] which also increases the density of radicals favorable for nitriding process. As the argon concentration increases, the sputtering rate increases which facilitates the diffusion of nitrogen resulting in the formation of silicon nitride films. On the other hand, during higher sputtering rate (higher reaction rate), the nucleation of Si_3N_4 should be maximum but the formation of amorphous film (for 90%Ar) indicating that the high sputtering yield is not favorable to produce significant reaction between the plasma species. Due to more collisions, plasma species have low energy and therefore hinders the growth of crystalline films or low concentration of available nitrogen (10%) may be the other reason.

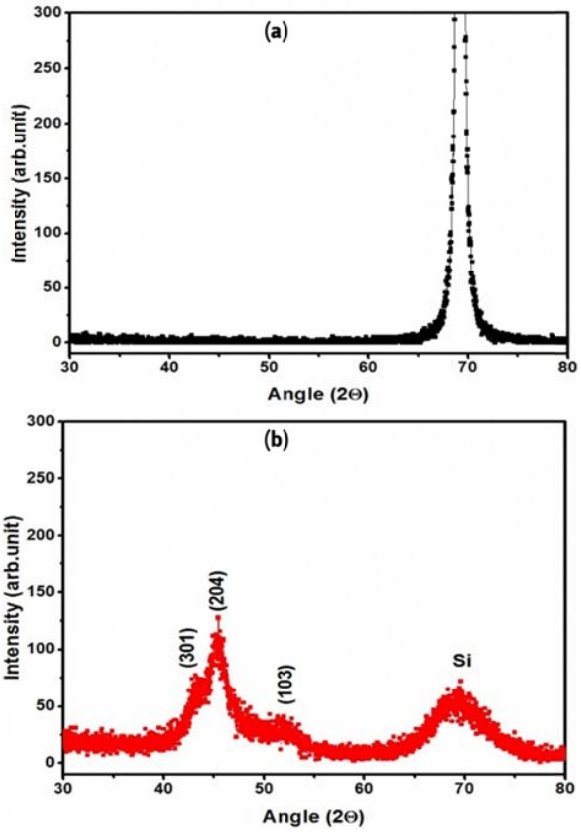

Fig. 2 The XRD patterns of untreated and nitrided Si layer for different N_2-Ar concentrations (a) Untreated Si (b) 70%N_2 + 30%Ar

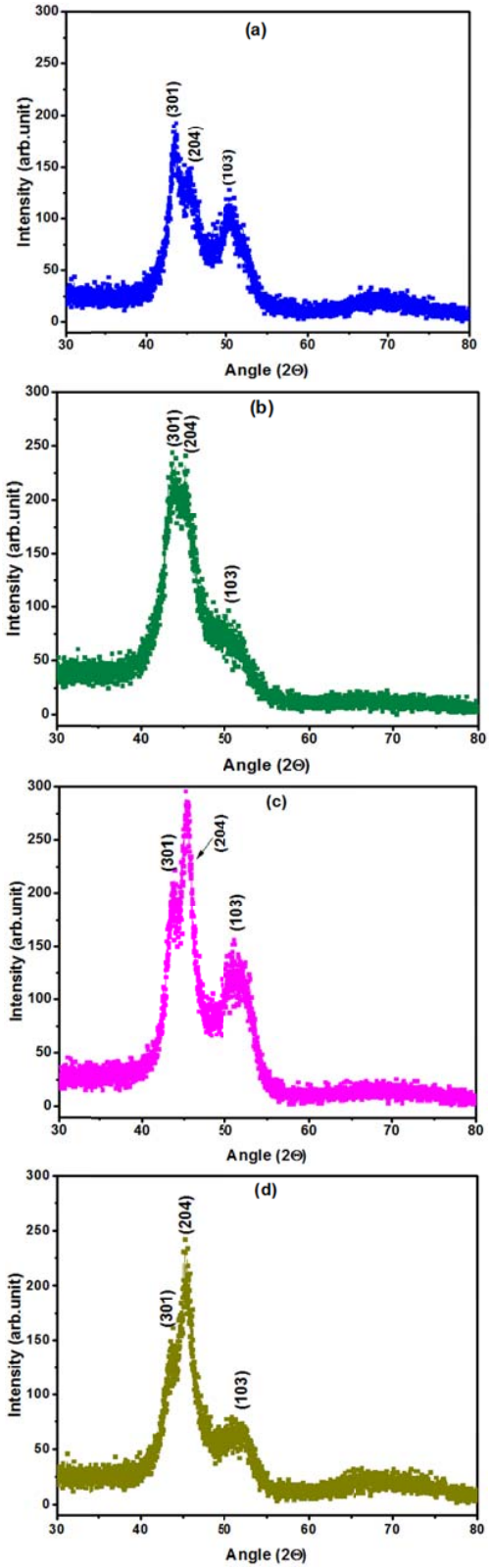

Fig. 3 The XRD patterns of nitrided Si layer for different N_2-Ar concentrations (a) 60%N_2 + 40%Ar (b) 50%N_2 + 50%Ar (c) 40%N_2 + 60%Ar (d) 30%N_2 + 70%Ar

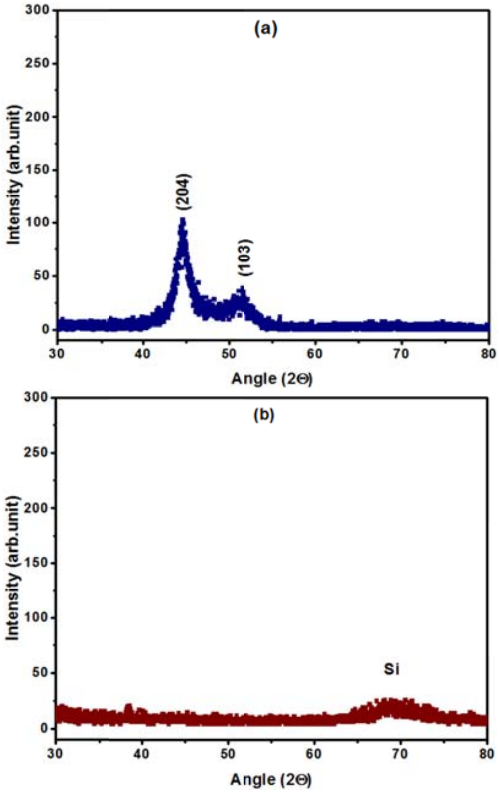

Fig. 4 The XRD patterns of nitrided Si layer for different N_2-Ar concentrations (a) 20%N_2 + 80%Ar (b) 10%N_2 + 90%Ar

The XRD results indicate that the nucleation of Si_3N_4, their growth and the development of residual stresses are directly influenced by the variation of N_2-Ar concentrations.

B. Residual Stress Analysis

Figs. 7-9 represent the de-convolution of XRD patterns in order to calculate the residual stress induced in the nitride layer and crystallite size. The de-convolution of the overlapped diffraction peaks has been performed using Gaussian distribution function.

Fig. 5 demonstrates the residual stresses developed in the nitrided layers by using XRD data. The diffraction peaks show up and down shifting from their stress free data indicating the presence of residual stresses. During nitriding process, a sufficient amount of energy is transferred to the substrate surface by the bombardment of energetic ions/electrons/radicals results in the increase of substrate surface temperature which causes to nucleate new phases and their growth. The incorporation of impurity atoms/molecules/radical interstitially causes to distort the substrate lattice which changes the d-values. This change in d-values will change the lattice parameters results in change of crystal structure and surface morphology of the nitrided layers.

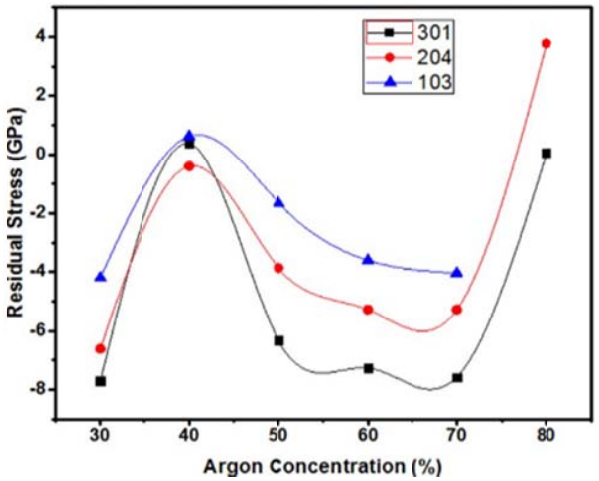

Fig. 5 Variation in residual stress using different argon concentration

It is well known that the increase in substrate surface temperature and lattice distortion developed during ions bombardment change the inter-atomic distance and thermal expansion coefficients [21]. The tensile stress develops due to down-shifting of diffraction planes whereas compressive stress results due to up-shifting of diffraction planes [22]. The actual residual stress can be estimated by the strain produced in the nitride layer, given by [23]:

$$\varepsilon = \frac{(do-d)}{d} \quad (1)$$

where d_o and d are the observed and standard value of d-spacing. The multiplication of strain with elastic constant (Si_3N_4) gives the value of residual stress [24].

$$\text{Residual stress} = \varepsilon * E \quad (2)$$

The elastic constant (E) of Si_3N_4 is found to be 400 GPa [25].

Fig. 5 exhibits the residual stresses developed in Si_3N_4 layers show the cyclic behavior for Ar concentration ranged from 30% to 80%. It is found that the residual stress changes from -7.80 GPa to 3.85 GPa with the increase of Ar concentration in N_2-Ar plasma. This is due to increase in Ar concentration which increases total energy deliverance to silicon substrate surface. This, in turn, results in the increase of silicon temperature which will increase the nucleation rate of new phases. For 30% Ar, the stresses developed in Si_3N_4 (103), (301) planes are compressive in nature which transformed to tensile for 40% Ar. The tensile stress is observed in the above mentioned diffraction planes again transformed to compressive stress which increases up to 70% Ar. However, different diffraction planes have different stress values (Fig. 6). For 80% Ar, the compressive stresses in Si_3N_4 (204) and (301) planes are again transformed to tensile.

It is concluded that the stress transformation in different planes of Si_3N_4 phases strongly depend on increasing Ar concentrations in N_2-Ar plasma.

C. Crystallite Size Analysis

The average crystallite size of the silicon nitride layer can be calculated from XRD data using Scherer's formula

$$\text{Crystallite size} = \frac{k\lambda}{\text{FWHM}\cos\theta} \quad (3)$$

where k is a constant having a value in the ranged from 0.9 to 1, depending on the cell geometry. λ is the wavelength of radiation (1.5406 ºA), FWHM is the full width half maxima of the corresponding diffraction peak, and θ (radian) is the Bragg's angle.

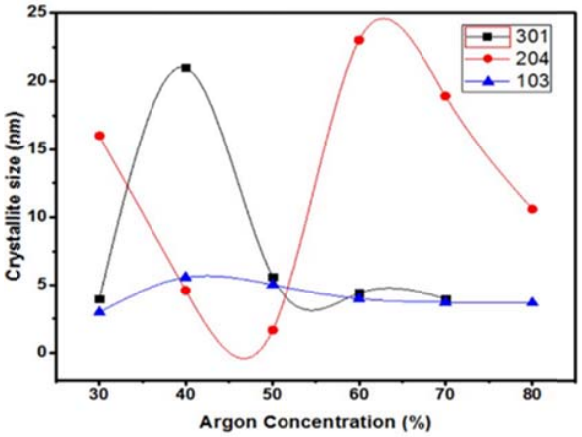

Fig. 6 The variation of crystallite size with Ar concentration in N_2 plasma

Fig. 6 illustrates the variation of crystallite size with Ar concentration in N_2-Ar plasma. It can be clearly observed that the average crystallite size of different diffraction planes strongly depends on Ar concentration. The crystallite size of (204) plane is minimum for 50% Ar, whereas it is the maximum for 60% Ar concentration. Interestingly, a little bit change in the crystallite size of (103) diffraction plane is observed with increasing Ar concentration. It means that the broadening of different diffraction planes shows different trend with variation in Ar concentration.

It is well known that there is a competition between diffusion and sputtering processes by the energetic ions or atoms of Ar and N_2. Moreover, higher the energetic ions concentration, higher will be the nucleation which affects the diffusion of N_2 species and results in the increase of peak broadening. It will decrease the crystallite size of different plane with increasing Ar concentration [26]-[28].

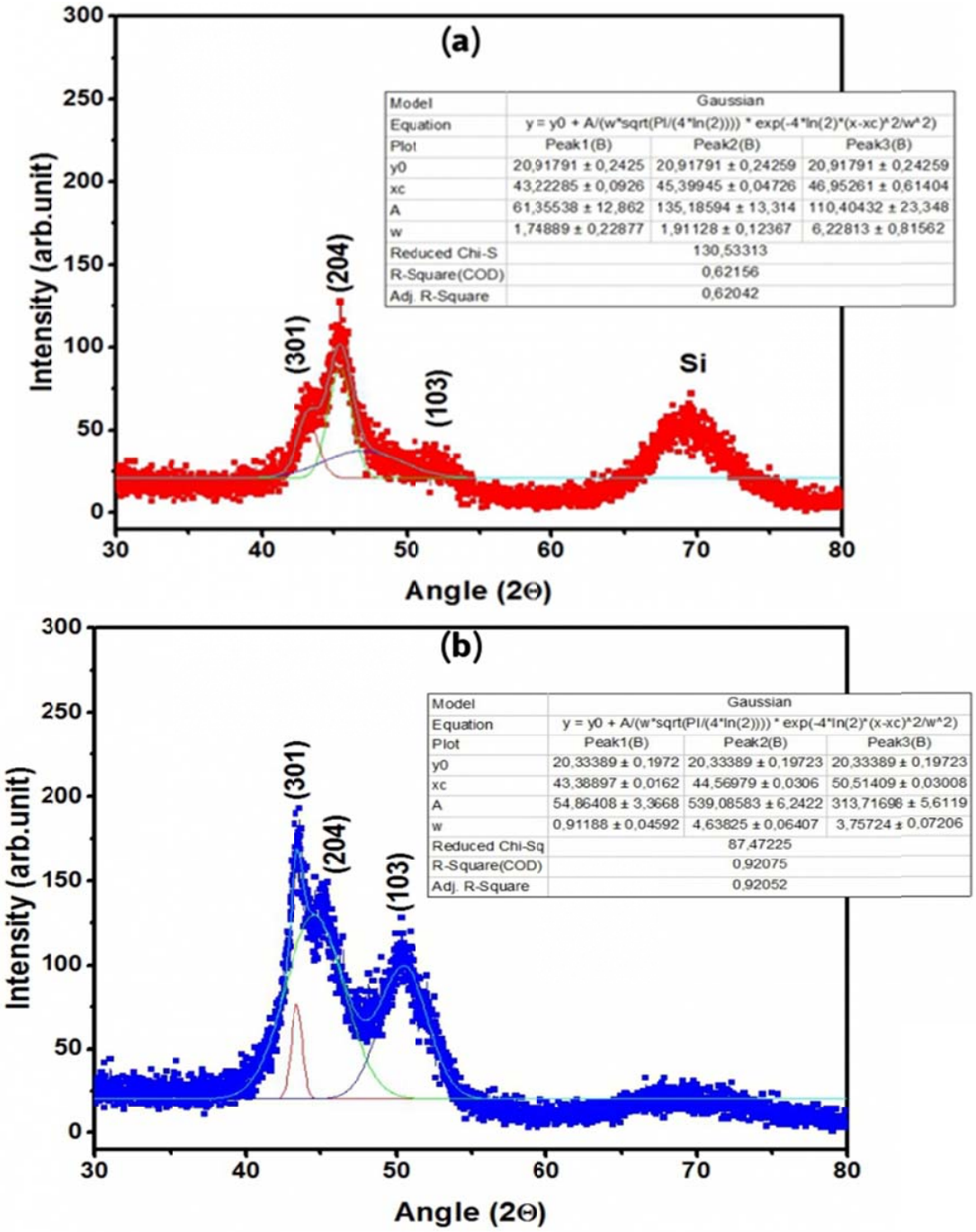

Fig. 7 De-convolution of the overlapped diffraction peaks using Gaussian distribution function for (a) 70%N_2 + 30%Ar (b) 60%N_2 + 40%Ar

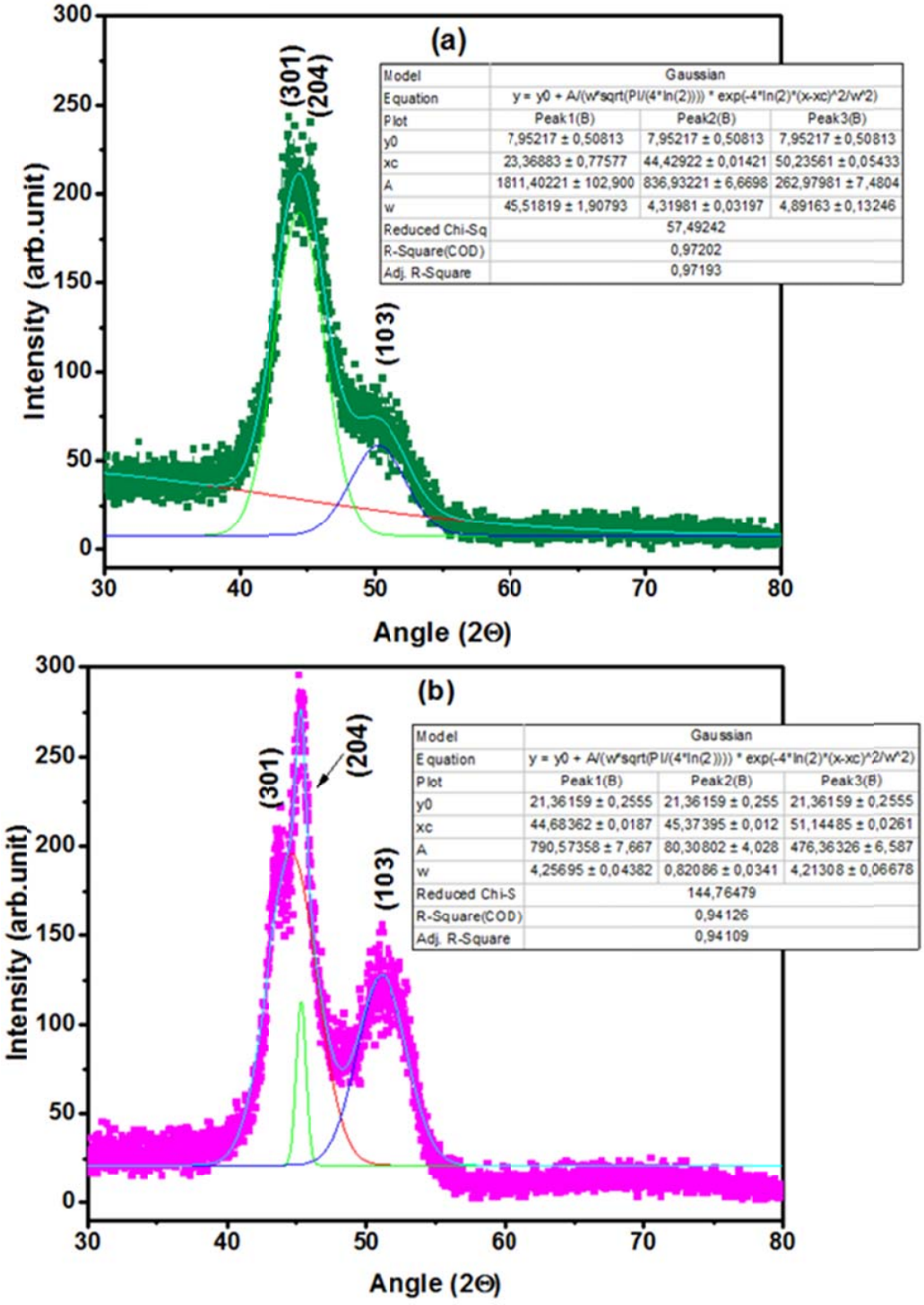

Fig. 8 De-convolution of the overlapped diffraction peaks using Gaussian distribution function for (a) 50%N_2 + 50%Ar (b) 40%N_2 + 60%Ar

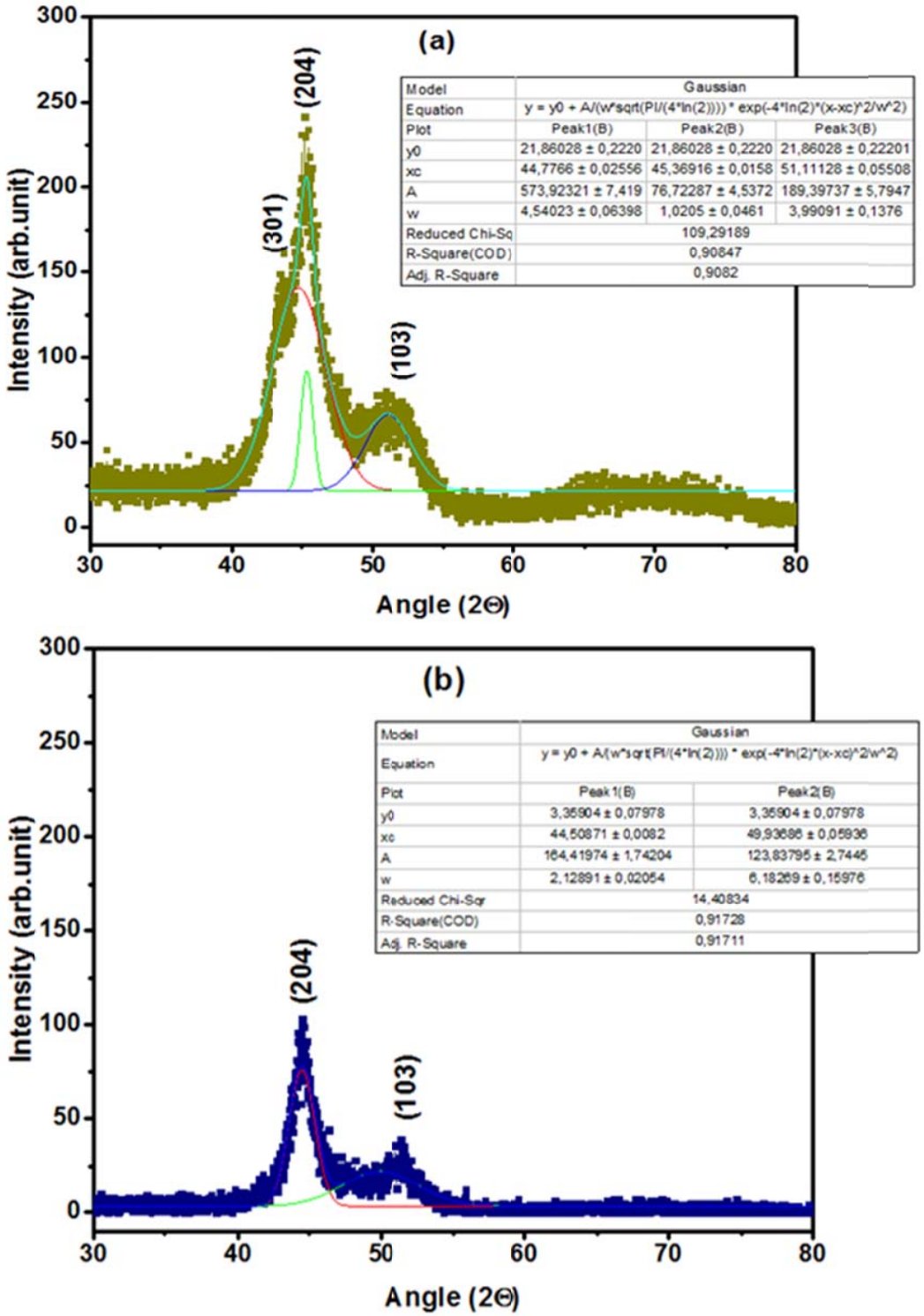

Fig. 9 De-convolution of the overlapped diffraction peaks using Gaussian distribution function for (a) 30%N_2 +70%Ar (b) 20%N_2 + 80%Ar

D.FTIR Analysis

The FTIR analysis provides information regarding the compositional and vibrational properties of the nitrided layers. Fig. 10 elaborates the FTIR spectrum of Si3N4 film nitrided for 40% N2 and 60% Ar concentration.

It is also reported that the Si–N bond is sensitive to oxygen content; even small oxygen content changes the film composition resulting in the formation of SiON film instead of

Si_3N_4 film which is responsible for the shifting of Si–N bond position towards higher wave number [5].

The vibration frequency of a chemical bond is directly related to the electronegativity of the nearest neighbors. Electron clouds in a bond tend to orient themselves towards the more electronegative atom involved in the bond. This effect is known as induction effect. So, oxygen atoms incorporated in the nitrided layer produces induction effect over Si-N bonds. Nitrogen atoms are replaced by oxygen atoms, which are more electronegative decreasing the bond length.

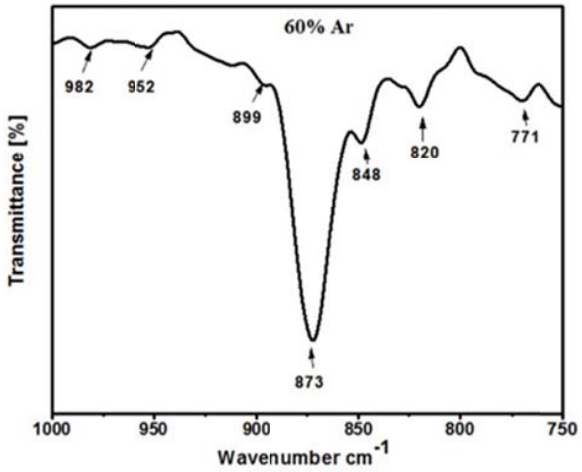

Fig. 10 The FTIR spectrum of silicon sample nitrided for 40% N_2 and 60% Ar plasma

The vibrational frequency associated with the bonding group shows a broad Si–N bond at about 771–985 cm^{-1} which is attributed to the asymmetric Si–N bond-stretching vibration mode [29], [32]. Vila et al. [30], [31] have reported that the Si–N peak in Si_3N_4 films lies in the range from 700–1200 cm^{-1}. The Si–N peak appears at 873 cm^{-1} matches well with the reported value [5]. Moreover, small overtones/peaks observed at about 771, 820 and 840 cm^{-1} are attributed to Si–N vibrational bond. It is examined from the FTIR transmission spectrum of Si_3N_4 film that the number of emission bands and their energy represented by bond strength are strongly affected by the Ar concentration in N_2-Ar plasma.

E. OM Analysis

Figs. 11 and 12 show the optical micrographs (×500 magnifications) of untreated and nitrided sample of Si for different N_2-Ar plasma. The surface morphologies of untreated Si and nitrided films for different Ar concentration are significantly different. The pores of different diameter are observed in the film. However, the numbers of pore are different in different nitrided films along with the formation of bubbles of irregular diameters. For 60% Ar illustrated in Fig. 12 (a), a crack free film covered with large numbers of nodules [33] is observed. This is due to higher sputtering and diffusion rates which increase the reaction possibilities of N_2 with Si. The results show that one can obtain a particular surface morphology of the nitrided film depending on the Ar concentration in N_2-Ar plasma.

F. SEM Analysis

Figs. 13 and 14 show the surface morphologies of untreated and nitrided layers. For 30% Ar, the surface morphology of nitrided layer indicates the formation of nano-particles of different shapes and size and the up and down regions show the formation of rough surface as shown in Fig. 13 (b). For 40% Ar, network microstructure is observed with nanoparticles sparsely spread in the background as represented in Fig. 13 (c). However, the surface roughness of nitrided layer is comparatively low. A careful investigation reveals that the surface morphologies of nitrided layers strongly depend on the Ar concentration. Moreover, highly rough surface is observed for 60% Ar as clearly shown in Fig. 14 (a), whereas it is smooth comparatively for 70% Ar concentrations. Additionally, totally surface appearance is changed for 90% Ar concentration showing the formation of long nano-rods and the deposited film is compact in nature. This change in surface appearance and roughness is due to the difference in diffusivity of N_2 along the grain boundary sites and Si lattice. We hypothesize that the increasing Ar concentration in N_2-Ar plasma enhances the diffusion rate of N_2 in Si lattice which increases the ionization and concentration of the active species and results in the change in surface microstructure.

The SEM cross sectional view of the nitrided layer gives the information about the film thickness. The film thickness (d) is used to calculate the diffusion rate of N_2 with increasing Ar concentration. Using the thickness data from cross-sectional image and by using the relation given below, the diffusion rate can be obtained [34].

$$\text{Diffusion rate} = d^2/t \quad (4)$$

where d is the thickness of the nitrided layer, and t is the treatment time.

Fig. 15 shows the relation between the diffusion rates of N_2. It is found that the diffusion rate strongly depends on Ar concentration.

With increasing Ar concentration, the number of active species and electron number density increases, which in turn increases the substrate temperature. This temperature is sufficient to nucleate the Si_3N_4 around the grain boundaries. For the samples that are nitrided at 70-90% Ar concentration, the active species and electron number density reaches maximum but due to collisions, energy (temperature) of the particles decreases which in turn decreases the diffusion of N_2 species in Si lattice.

G.AFM Analysis

The AFM images of untreated Si and Si_3N_4 films for different Ar concentration are shown in Figs. 17-20. The outlook appearance of the AFM images confirms that the surface morphology depends on Ar concentration.

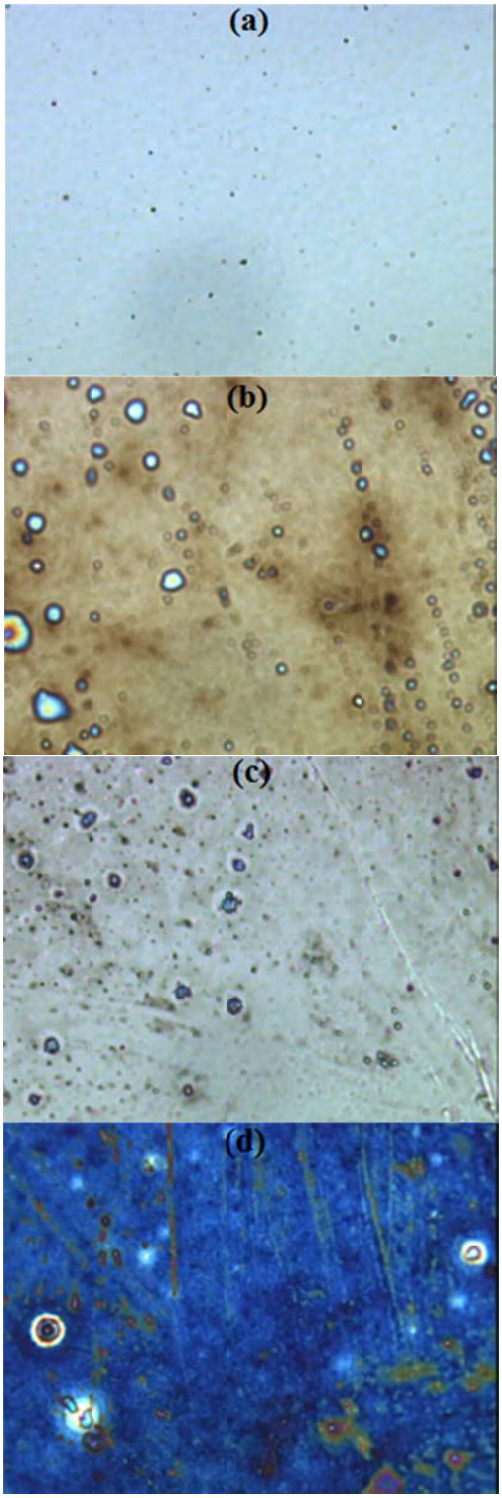

Fig. 11 The optical micrographs (Magnification×500) of untreated Si and nitrided Si samples (a) Untreated Si (b) 70%N_2 + 30%Ar (c) 60%N_2 + 40%Ar (d) 50%N_2 + 50%Ar

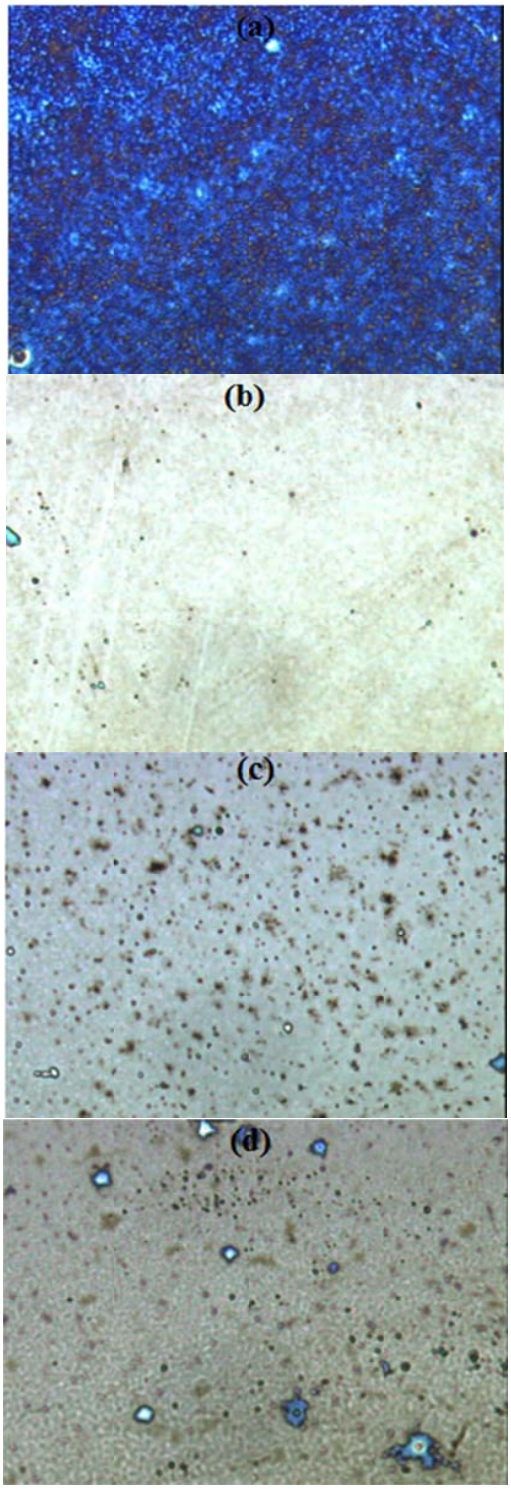

Fig. 12 The optical micrographs (Magnification×500) of nitrided Si samples (a) 40%N_2 + 60%Ar (b) 30%N_2 + 70%Ar (c) 20%N_2 + 80%Ar (d) 10%N_2 + 90%Ar

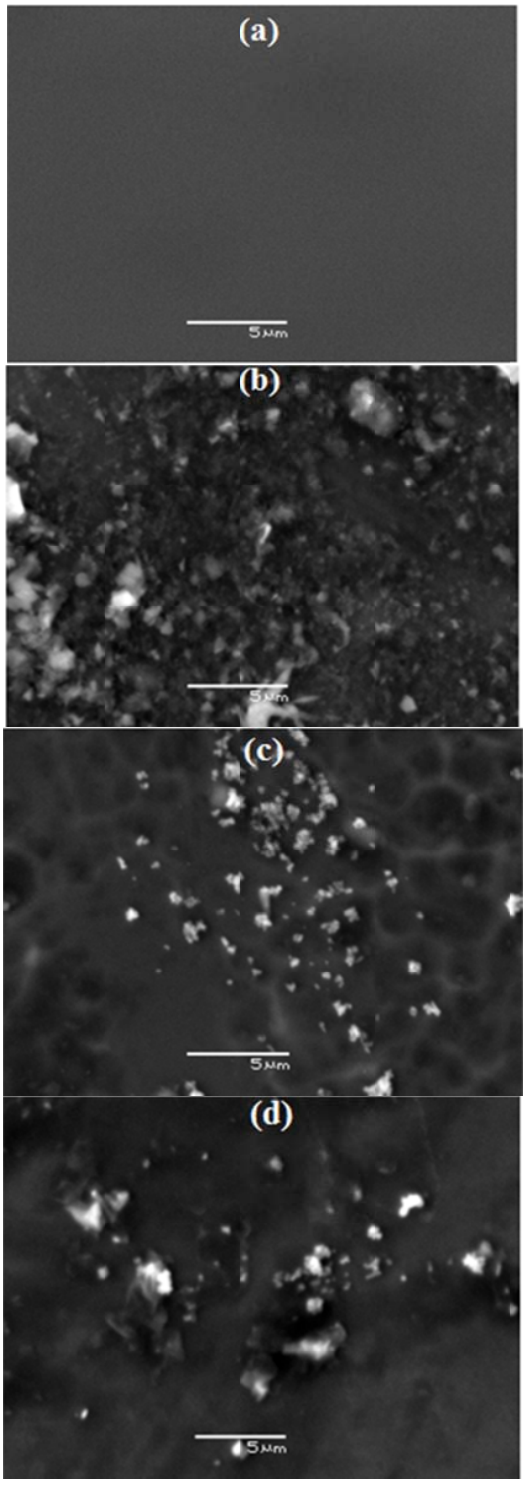

Fig. 13 The SEM micrographs (×5000 Magnification) of untreated and nitrided Si (a) Untreated Si (b) 70%N_2 + 30%Ar (c) 60%N_2 + 40%Ar (d) 50%N_2 + 50%Ar

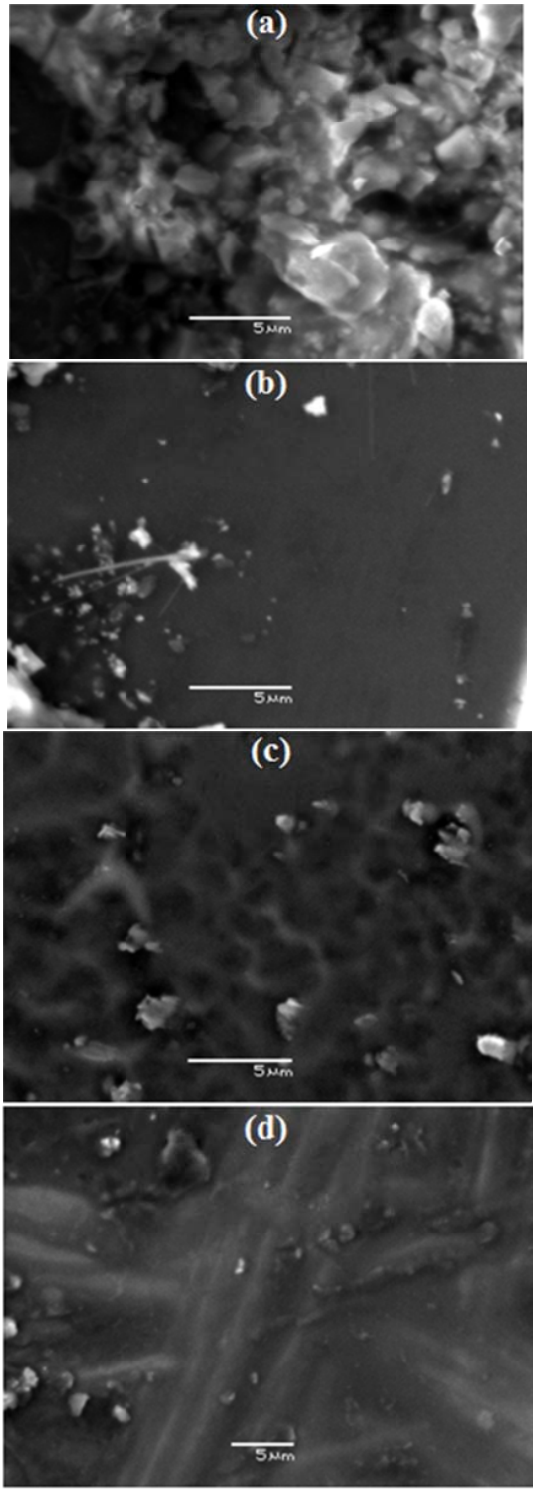

Fig.14 The SEM micrographs (×5000 Magnification) of nitrided Si (a) 40%N_2 + 60%Ar (b) 30%N_2 + 70%Ar (c) 20%N_2 + 80%Ar (d) 10%N_2 + 90%Ar

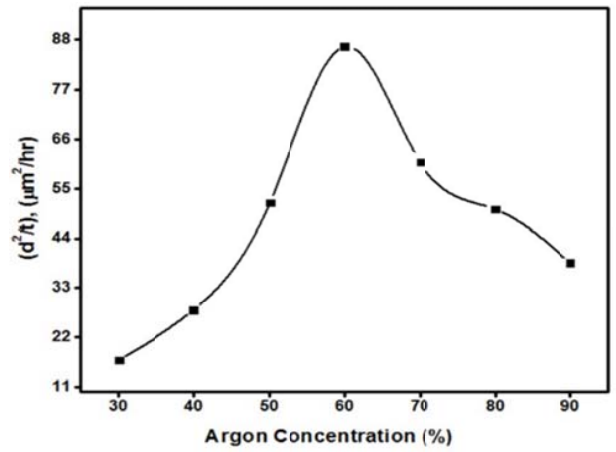

Fig. 15 Diffusion rate of nitrogen as a function of Ar concentration at treatment time 4 h

For 30% to 70% Ar concentration, the vertical droplets of different heights are observed. There is a small change in droplet heights. Therefore, the nitrided film which is rough is agreed well with the SEM analysis. The height and distribution of these droplets depend on the Ar concentration in N_2-Ar plasma.

The size of solid droplet increases with increasing the Ar concentration which increases surface roughness of the nitrided layers. The present work highlights that the surface morphology and surface roughness are associated with Ar concentration. Moreover, the researchers have pointed out that the nucleation and growth rate of nitrided layer strongly depend on Ar concentration [35].

In the present work, the XRD, SEM and AFM analysis again confirm the nucleation and growth rate of nitrided films which are attributed with the increase of Ar concentration. Additionally, for 90% Ar concentration, the nucleation, growth rate and surface roughness of the nitrided layer are reduced which is due to higher sputtering rate of the substrate surface, which provides the smooth growth of nitrided layer.

The variation in surface roughness with increasing Ar concentration in N_2-Ar plasma is shown in Fig. 16.

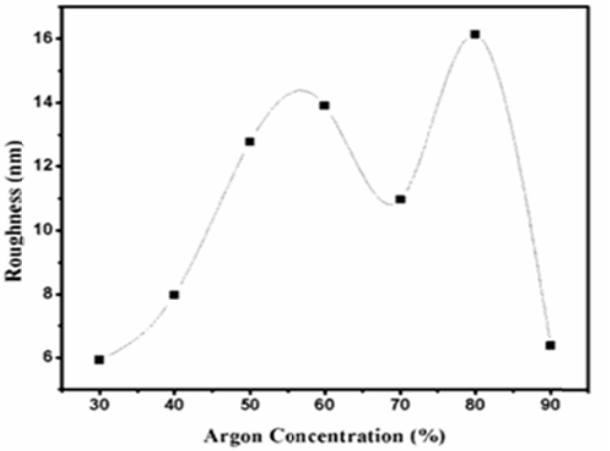

Fig. 16 The surface roughness of the nitrided Si films as a function of Ar concentration

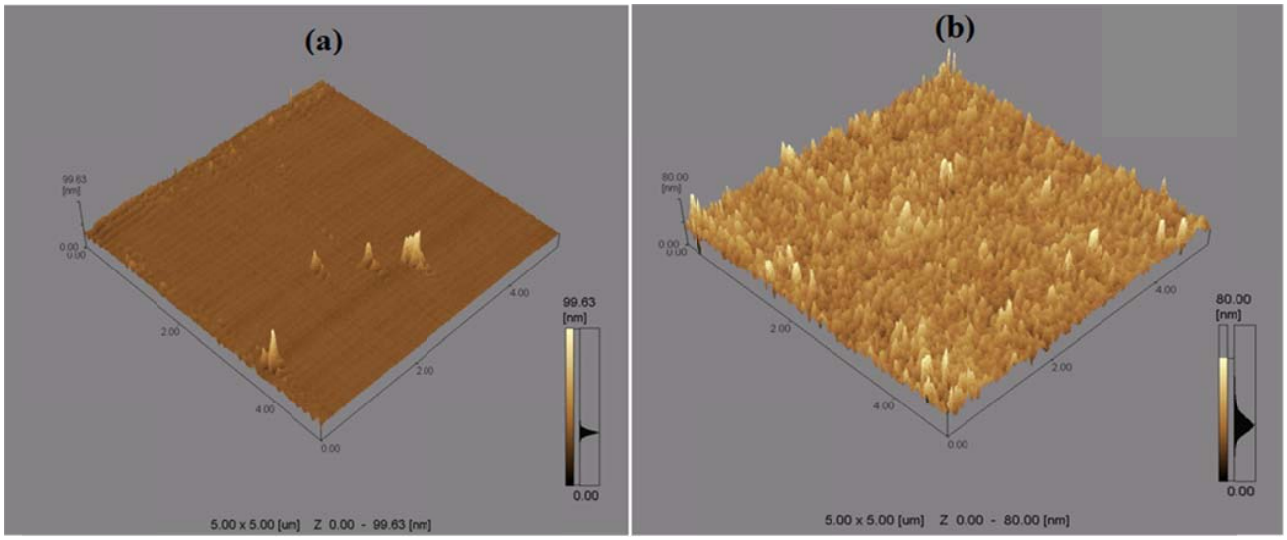

Fig. 17 The AFM images of untreated Si and Si_3N_4 films for different Ar-N_2 plasma. (a) Untreated Si (b) 70%N_2 + 30%Ar

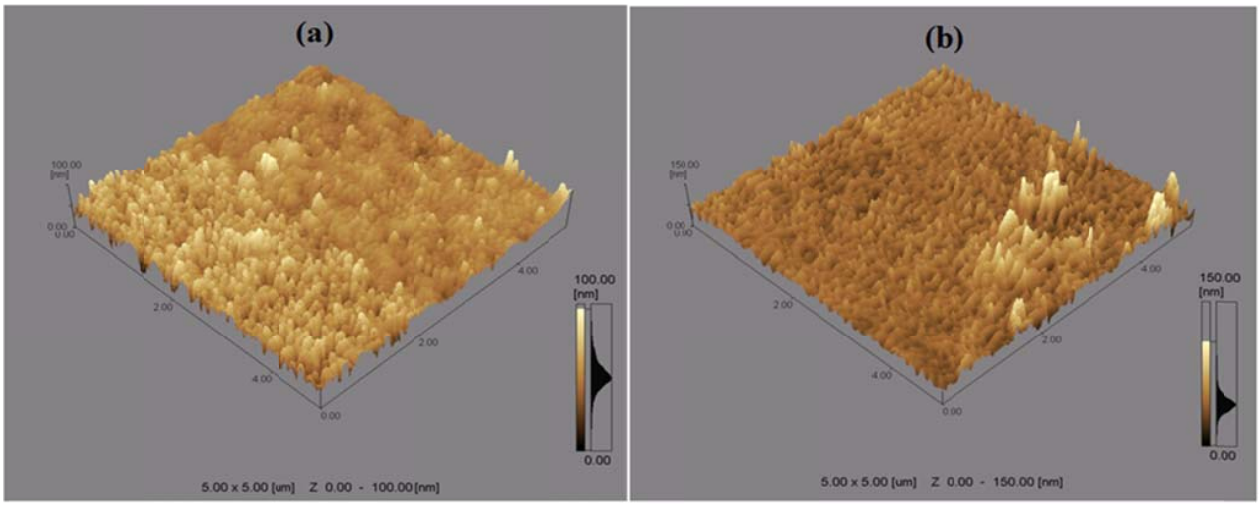

Fig. 18 The AFM images of Si_3N_4 films for different Ar-N_2 plasma. (a) 60%N_2 + 40%Ar (b) 50%N_2 + 50%Ar

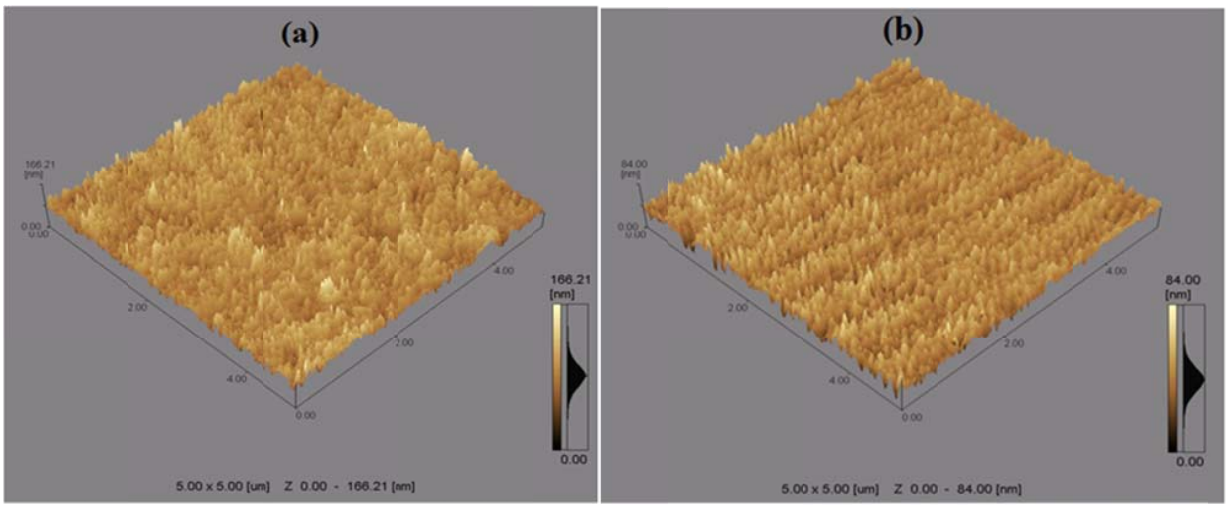

Fig. 19 The AFM images of Si_3N_4 films for different Ar-N_2 plasma. (a) 40%N_2 + 60%Ar (b) 30%N_2 + 70%Ar

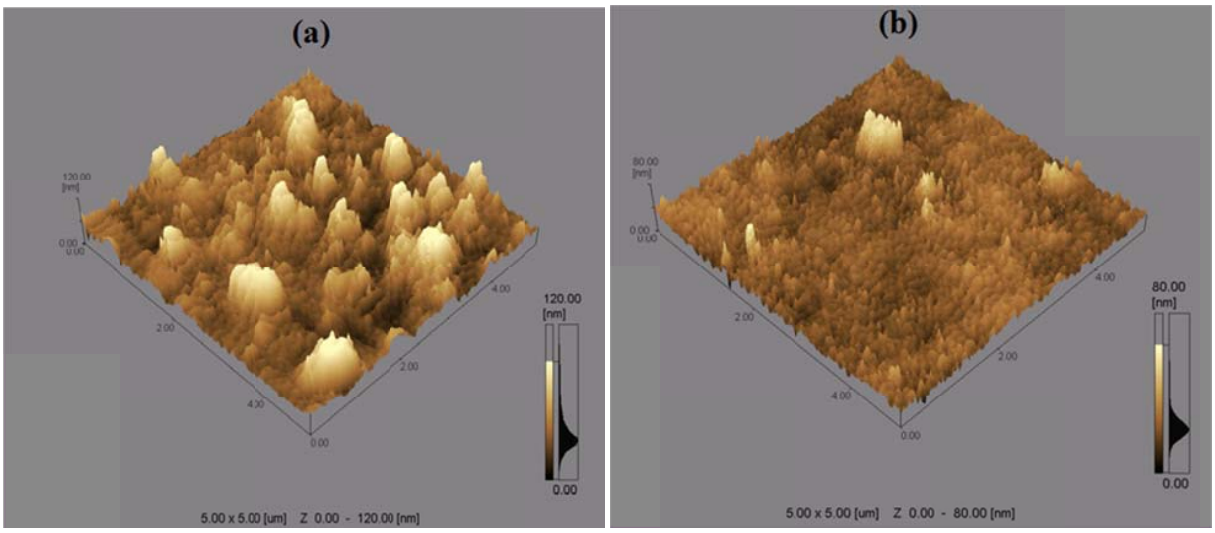

Fig. 20 The AFM images of Si_3N_4 films for different Ar-N_2 plasma (a) 20%N_2 + 80%Ar (b) 10%N_2 + 90%Ar

IV. Conclusions

The present work highlights that the active species generations (argon as sputtering gas) play an important role in the nitriding of silicon using 100 Hz pulsed DC glow discharge. The XRD results confirm the formation of Si_3N_4 films. The intense polycrystalline Si_3N_4 film is formed at 40% N_2 and 60% Ar plasma. The FTIR result highlights the formation of asymmetric Si_3N_4 film and the bond strength between Si and N species strongly depends on argon concentration in N_2-Ar plasma. The OM microstructure reveals the formation of nodules which are associated with the nucleation and growth of the nitrided layer. The SEM microstructure results show the formation of hills of nano-clusters of Si_3N_4 films. The AFM images relate the surface roughness of the nitrided layers formed for different Ar concentrations in N_2-Ar plasma. The peak–to-valley height (166.21 nm) is maximum for 60% Ar concentration. It is concluded that the crystallinity, crystallite size, residual stresses, bond strength, surface morphology, particle shape and size, particle distributions, formation of hills of clusters and cluster of nanoparticles are associated with Ar concentration in N_2-Ar plasma. Up to 60% Ar concentration in N_2-Ar plasma is most suitable for the nitriding of silicon due to the production of large number of active species and higher temperatures are achieved.

References

[1] H. Klemm, "Silicon nitride for high-temperature applications," *J. Am. Ceram. Soc.,* vol. 93, pp. 1501–1522, 2010.

[2] W. Xu, B. Li, T. Fujimoto, I. Kojima, "Gas flow effects on the structure and composition of SiN /Si/SiNx films prepared by radio-frequency magnetron sputtering," *J. Mater. Res.,* vol. 16, pp. 308-313, 2001.

[3] A. Batan, A. Franquet, J. Vereecken, F. Reniers, "Characterization of the silicon nitride thin films deposited by plasma magnetron," *Surface and Interface Analysis,* vol. 40, pp. 754–757, 2008.

[4] V. Pavarajarn, S. Kimura S, "Roles of hydrogen and oxygen in the direct nitridation of silicon," *Ind Eng Chem Res.,* vol. 42, pp. 2434-2440, 2003.

[5] S. J. Patil, S. A. Gangal, "Activated reactive evaporation deposited silicon nitride as a masking material for MEMS fabrication," J. Micromech. Microeng., vol. 15, pp. 1956–1962, 2005.

[6] Y. Kuo, H. H. Lee, "Plasma enhanced chemical vapor deposition of silicon nitride below 250˚C," *Vacuum*, vol. 66, pp. 299-303, 2002.

[7] J. Yang, R. C. Guzman, S. O. Salley, K. Y. Simon, B. H. Chen, M. M. C. Cheng, "Plasma enhanced chemical vapor deposition silicon nitride for a high-performance lithium ion battery anode," *Journal of Power Sources*, vol. 269, pp. 520-525, 2014.

[8] T. C. Tsai, L. R. Lou, C. T. Lee, "Influence of deposition conditions on silicon nanoclusters in silicon nitride films grown by Laser-Assisted CVD Method," *IEEE Transactions on nanotechnology,* vol. 10, pp. 197-202, 2011.

[9] I. A. Khan, R.S. Rawat , R. Verma, G. Macharaga, R. Ahmad, "Role of charge particles irradiation on the deposition of AlN films using plasma focus device," *Journal of Crystal Growth,* vol. 317, pp. 98–103, 2011.

[10] A. Bogaerts, E. Neyts, R. Gijbels, J. V. Mullen, "Gas discharge plasmas and their applications," *Spectrochimica Acta*, vol. 57B, pp. 609-658, 2002.

[11] M. Moradshahi, T. Tavakoli, S. Amiri, S. Shayeganmehr, "Plasma nitriding of Al alloys by DC glow discharge," *Surface & Coatings Technology*, vol. 201, pp.567–574, 2006.

[12] J. Liu, F. Sun, H. Yu, "Enhancement of the molecular nitrogen dissociation and ionization levels by argon mixture in flue nitrogen plasma," *Curr Appl Phys.,* vol. 5, pp. 625-628, 2005.

[13] M. Tabbal, M. Kazpoulo, T. Chritidis, S. Isber, "Enhancement of the molecular nitrogen dissociation levels by argon dilution in surface-wave-sustained plasmas," *J Appl Phys.,* vol. 78, pp. 2131, 2001.

[14] M. A. Naveed, A. Qayyum, A. Shujaat, M. Zakaullah, "Effects of helium gas mixing on the production of active species in nitrogen plasma," *Physics Letters A,* vol. 359, pp. 499-503, 2006.

[15] A. Saeed, A. W. Khan, M. Shafiq, F. Jan, M. Abrar, M. Zakaulislam, M. Zakaullah, "Investigation of 50 Hz pulsed DC nitrogen plasma with active screen cage by trace rare gas optical emission spectroscopy," *Plasma Science and Technology,* vol. 16, pp. 324-328, 2014.

[16] P. G. Reyesa, C. Torresa, H. Martínez, "Electron temperature and ion density measurements in a glow discharge of an Ar–N_2 mixture," *Radiation Effects & Defects in Solids,* vol. 169, pp. 285–292, 2014.

[17] F. U. Khan, N. U. Rehman, S. Naseer, M. Y. Naz, N. A. D. Khattak, M. Zakaullah, "Effect of excitation and ibrational temperature on the dissociation of nitrogen molecules in Ar-N2 mixture RF discharge," *Spectroscopy Letters,* vol. 44, pp. 194–202, 2011.

[18] M. Quast, P. Mayer, H. R. Stock, H. Podlesak, B. Wielage, "In situ and ex situ examination of plasma-assisted nitriding of aluminium alloys," Surf Coat Technol., vol. 135, pp. 238-249, 2001.

[19] M. K. Sharma, B. K. Saikia, S. Bujarbarua, "Optical emission spectroscopy of DC pulsed plasmas used for steel nitriding," Surface & Coatings Technology, vol. 203, pp. 229–233, 2008.

[20] Z. Wronski, "Dissociation of nitrogen in the plasma-cathode interface of Glow discharges," *Vacuum,* vol. 78, pp. 641-647, 2005.

[21] K. Kusaka, D. Taniguchi, T. Hanabusa, K. Tominaga, "Effect of input power on crystal orientation and residual stress in AlN film deposited by dc sputtering," Vacuum, vol. 59, pp. 806-813, 2000.

[22] R. S. Rawat, P. Arun, A. G. Vedeshwar, P. Lee, S. Lee, "Effect of energetic ion irradiation on CdI_2 films," *J Appl Phys.,* vol. 95, pp. 7725 – 7730, 2004.

[23] P. Tyagi, R. K. Mishra, N. C. Mehra, A. G. Vedeshwar, "Dependence of optical band gap on residual stress in group IIB Iodide (ZnI_2, CdI_2, HgI_2) films," Integr Ferroelectr., vol. 122, pp. 52-62, 2010.

[24] C. Sarioglu, U. Demirler, M. K. Kazmanli, M. Urgen, "Measurement of residual stresses by x-ray diffraction techniques in MoN and Mo2N coatings deposited by arc PVD on high-speed steel substrate," *Surf Coat Technol.,* vol. 190, pp. 238-243, 2005.

[25] D. F. Moore, R. M. Bostock, P. Boyl, E. H. Conradie, "Materials issues in the application of silicon nitride films in silicon MEMS," *MRS Fall Meeting,* 687, 2001.

[26] J. J. Olaya, S.E. Rodil, S. Muhl, E. Sanchez, "Comparative study of chromium nitride coatings deposited by unbalanced and balanced magnetron sputtering," Thin Solid Films, vol. 474, pp. 119-126, 2005.

[27] A. Barata, L. Cunha, C. Moura, "Characterisation of chromium nitride films produced by PVD techniques," Thin Solid Films vol. 398-399, pp. 501-506, 2001.

[28] K. Nunan, G. Ready,P. Garone, G. Sturdy, J. Sledziewski, "Developing a manufacturable process for the deposition of thick polysilicon films for micro machined devices," IEEE/SEMI Advanced Semiconductor Manufacturing Conference 0-7803-5921-6/00/$10.00 0 2000 IEEE, pp. 357-366, 2000.

[29] E. Tomasella, F. Rebib, M. Dubois, J. Cellier, M. Jacquet, "Structural and optical properties studies of sputtered a-SiCN thin films," *Journal of Physics Conference Series*, vol. 100, pp. 082045, 2008.

[30] M. Vila, C. Prieto, P. Miranzo, M. I. Osendi, R. Ramırez, "Characterization of Si_3N_4 thin films prepared by r.f. magnetron sputtering," *Surface and Coatings Technology,* vol. 151 – 152, pp. 67–71, 2002.

[31] M. Vila, J. A. Gago, A. M. Martin, C. Prieto, P. Miranzo, M. I. Osendi, J. G. Lopez, M. A. Respaldiza, "Compositional characterization of silicon nitride thin films prepared by RF-sputtering," Vacuum, vol. 67, pp. 513–518, 2002.

[32] Y. Zhou, D. Probst, A. Thissen, E. Kroke, R. Riedel, R. Hauser, H. Hoche, E. Broszeit, P. Knoll, H. Stafast, "Hard silicon carbonitride films obtained by RF-plasma-enhanced chemical vapor deposition using the single-source precursor bis(trimethylsilyl) carbodiimide," *J. Eur. Ceram. Soc.,* vol. 26, pp. 1325-1335, 2006.

[33] A. Hassan, "Surface modification of metals using plasma torch," Proceedings of the 7th Conference on Nuclear and Particle Physics. Sharm El-Sheikh Egypt, pp. 595-603, 2009.

[34] F. M. El-Hossarry, "The influence of surface microcracks and temperature gradients on the rf plasma nitriding rate," Surf. Coat. Technol., vol. 150, pp. 277–281, 2002.

[35] L. Pranevicious, C. Templier, J. R. Riviere, P. Meheust, L. L. Pranevicius, G. Abrasonis, "On the mechanism of ion nitriding of an austenitic stainless steel," *Surf. Coat. Technol.,* vol. 135, pp. 250-257, 2001.